CSIRO PUBLISHING

www.publish.csiro.au/journals/ijwf *International Journal of Wildland Fire*, 2006, **15**, 517–525

Measurements of moisture in smoldering smoke and implications for fog

Gary L. Achtemeier

USDA Forest Service, Southern Research Station, Fire Sciences Laboratory, Athens, GA 30602, USA. Email: gachtemeier@fs.fed.us

Abstract. Smoke from wildland burning in association with fog has been implicated as a visibility hazard over roadways in the southern United States. A project began in 2002 to determine whether moisture released during the smoldering phases of southern prescribed burns could contribute to fog formation. Temperature and relative humidity measurements were taken from 27 smoldering 'smokes' during 2002 and 2003. These data were converted to a measure of the mass of water vapor present to the mass of dry air containing the vapor (smoke mixing ratio). Some smokes were dry with almost no moisture beyond ambient. Other smokes were moist with moisture excesses as large as 39 g kg^{-1}. Calculations show that ground-level smoke moisture excesses have no impact on ambient relative humidity during the day. However, the impact at night can be large enough to increase the ambient relative humidity to 100%. Therefore smoke moisture may be a contributing factor to the location and timing of fog formation.

Additional keywords: highway accidents; visibility.

Introduction

Land managers in the Southern United States (the South: an area including 13 states roughly from Texas to Virginia and from the Ohio River to the Gulf of Mexico) use prescribed fire to treat 6 to 8 million acres (2–3 million ha) of forest and agricultural lands each year (Wade *et al.* 2000). Although the vast majority of prescribed burns are carried out without incident, there are occasions when residual smoke combines with meteorological conditions to compromise visibility. Smoke from southern prescribed fires releases high concentrations of chemical compounds that can impact air quality and visibility (Ward and Hardy 1991). Kokkola *et al.* (2003) have shown that heavily polluted conditions can favor the formation of dense radiation fogs consisting of large numbers of relatively small droplets. These fogs can form when relative humidities are slightly less than 100%.

Multiple-vehicle pile ups, numerous physical injuries, extensive property damage, and fatalities have been associated with visibility reductions due to smoke or a combination of smoke and fog on roadways. Most serious accidents occur during the night or at sunrise as smoke trapped in stream valleys and basins drifts across roadways. Mobley (1989) conducted a comprehensive study on smoke-related highway incidents that occurred in the South from 1979 to 1988. During this period, Mobley found that visibility reduction caused by smoke or a combination of smoke and fog caused 28 fatalities, over 60 serious injuries, numerous minor injuries, and litigation expenses into the millions.

Lavdas (1996) developed the Low Visibility Occurrence Risk Index (LVORI) to identify weather conditions linked to fog and highway accidents. Lavdas and Achtemeier (1995) showed that LVORI had skill in discriminating between widespread fog and local radiation fogs – the latter being more closely linked to smoke- and fog-related highway accidents. More recently, Achtemeier (2005) developed an operational numerical wind model to predict the movement of ground-level smoke during the night. This model identifies where smoke and areas of high ambient relative humidity may be collocated over complex terrain typical of that with interlocking ridge–valley systems with elevation differences of the order of 100 m.

Although it is known that smoke reduces visibility, there remains a question of whether smoke moisture is a contributor to the visibility reduction. Potter (2005) showed that moisture of combustion released during the flaming stage of wildfires is sufficient to modify (through enhancing cumulus cloud formation within the smoke plume) plume dynamics to create feedbacks through atmospheric circulations, impacting fire behavior. The issue in the present study is whether moisture released during the smoldering stage of prescribed fires modifies the relative humidity near the ground sufficiently to

10.1071/WF05115 1049-8001/06/040517

increase the density of existing fog or to trigger fog formation where fog might otherwise not have occurred.

Materials and methods

The smoke moisture measurements were taken at three locations in the southern United States. On 6 March 2002, data were collected after an operational prescribed burn on 417 acres (167 ha) located on the Oconee National Forest in central Georgia. Then, on 18 March 2002, data were collected from smoldering smokes in the aftermath of an experimental prescribed burn on 1.6 acres (0.64 ha) at the Hitchiti Experimental Forest, also in central Georgia. Finally, on 12 February 2003, smoke moisture data were collected as part of experimental burns on two plots of 2.5 acres (1.0 ha) each at the Francis Marion National Forest located in south-eastern South Carolina. Fuel types at all three sites are open stands of loblolly pine (*Pinus taeda* L.). The more complex vegetation strata at the Francis Marion site are described in Achtemeier *et al.* (2006).

Post-prescribed burn smoke temperature and relative humidity data were collected for a total of 27 smoldering 'smokes'. A 'smoke' is defined as a tiny plume of smoke less than 30 cm across rising above a patch of smoldering fuel.

A HMP45C temperature and relative humidity probe (Vaisala, Boston, MA, USA) was inserted into each smoke from 0.5 to 1.0 m downwind from smoldering fuels to gain a continuous record of temperature and relative humidity. Periodic measurements of the ambient temperature and relative humidity also were taken. The operational temperature range was −40°C to +60°C. The response time for the relative humidity sensor was rated at 15 s. In addition, a 36-gauge type T Teflon-coated thermocouple (Omega Engineering, Stamford, CN, USA) was attached to the sensor. This instrument has an operational temperature range from −200°C to +350°C and an estimated sub-second response time. Figure 1 shows the instrument in a residual smoke coming from a smoldering stump in the aftermath of the 18 March 2002 prescribed burn. The temperature and relative humidity sensors are located at the tip of the probe. Data from the Vaisala instrument and the thermocouple were recorded at 5-s intervals on a data recorder (Campbell Scientific, Logan, UT, USA) attached to the opposite end of the pole supporting the instrument.

Problems with the Vaisala instrument resulted in the need to recreate sensor temperatures for 18 March 2002. Measurements taken of smokes on 6 March 2002 showed that the response of the Vaisala temperature sensor to rapid changes in temperature was approximately 5 min. Thus temperature measurements from the slow-response sensor were not collected on 18 March 2002. These data were collected with the fast-response thermocouple and the Vaisala relative humidity sensor. However, further analysis of the data showed that the relative humidity was being calculated from the fast-response moisture sensor programmed

Fig. 1. The instrument consisting of a Vaisala temperature and relative humidity probe and an attached thermocouple inserted in a smoke in the aftermath of a prescribed burn at the Hitchiti Experimental Forest on 18 March 2002.

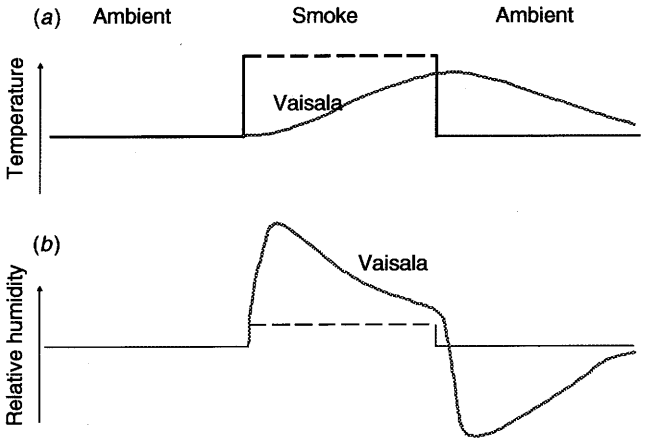

Fig. 2. A schematic showing how the coupling of the slow-response temperature sensor (*a*) to the fast-response moisture sensor (*b*) in the Vaisala instrument impacts relative humidity measurements of smoke. Solid and dashed lines represent ambient and smoke conditions, respectively.

with the slow-response temperature sensor. That meant that both the slow-response temperature and relative humidity measurements were not correct for short-term measurements.

Figure 2 shows schematically how the slow-response temperature sensor impacted relative humidity measurements. The black lines represent the true temperature and true relative humidity of the ambient air (solid black lines) and of the smoke (dashed lines). In this schematic, the temperature of the smoke is warmer than the temperature of the ambient air and the relative humidity of the smoke is greater than that for the ambient air. Initially, the ambient temperature and the

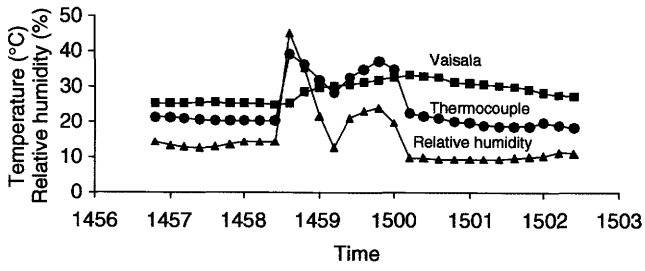

Fig. 3. Temperature (circles – thermocouple; squares – Vaisala) and relative humidity (triangles) for a smoke measured between 1457 and 1503 EST on 6 March 2002.

ambient relative humidity are measured correctly. When the instrument is inserted into the smoke, the slow-response sensor measures temperature along the solid line. Because the instrument-measured temperature is colder than the actual temperature of the smoke, the trace of the measured relative humidity is erroneously too high (Fig. 2*b*). As the temperature sensor slowly responds to the true smoke temperature, the relative humidity slowly decreases toward the correct value. Then, when the instrument is withdrawn from the smoke, the relative humidity trace spikes toward erroneously low values as the sensor-measured temperatures are now warmer than is the ambient temperature. The measured relative humidity gradually increases toward the correct value as the instrument temperature cools to the ambient temperature.

An example of relative humidity spikes for a smoke measured from 1457 to 1503 Eastern Standard Time (EST) on 6 March 2002 is shown in Fig. 3. The sensor was inserted into the smoke for ~1.5 min. The fast-response thermocouple, assumed to accurately measure both ambient and smoke temperature, is given by the line connecting circles. Temperatures of ~20°C (ambient) jumped to 40°C on insertion of the instrument into the smoke at 1458.5 EST. The temperature dropped to 28°C as a small eddy pushed the axis of the smoke to the side of the sensor, then rose again to 37°C shortly before 1500 EST. The sensor was withdrawn from the smoke at 1500 EST and the temperature dropped from 35 to 20°C.

By contrast, the slow-response temperature (line connecting squares) trace was a slow rise from 25°C on insertion into the smoke to 33°C when the sensor was withdrawn. The relative humidity (triangles) initially spiked from 13 to 45% (see Fig. 2 discussion). Relative humidity was ~20% (1459–1500 EST) when the slow-response sensor and the thermocouple measured temperatures in closer agreement. Note the relative humidity fall to 9% (the downward spike) on withdrawal of the sensor from the smoke after 1500 EST.

Given the connection between the fast-response humidity sensor and the slow-response temperature sensor in the Vaisala instrument, it was necessary to recreate the missing slow-response temperature in order to calculate smoke moisture for 18 March 2002. Temperatures measured by the fast-response thermocouple were assumed to be correct and

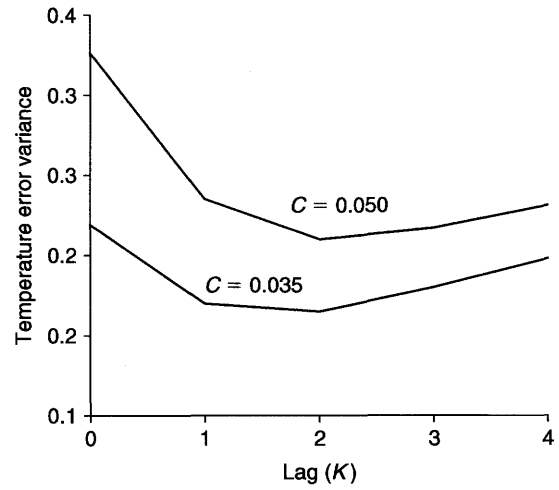

Fig. 4. The distribution of error variance as a function of lag for $C = 0.050$ and $C = 0.035$.

are the baseline for the calculations. The slow-response sensor temperatures are related to the baseline temperatures via

$$T_s^t = T_s^{t-1} + C[f(T_B) - T_s^{t-1}], \quad (1)$$

where the subscript '*s*' refers to the slow-response sensor and the subscript '*B*' refers to the baseline temperature. The function $f(T_B)$ must be both a smoothing and lag function to create the temperature record shown in Fig. 2. Let $f(T_B)$ take the following form so that Eqn 1 becomes:

$$T_s^t = T_s^{t-1} + C\left[\frac{1}{K+1}\sum_{k=1}^{K} T_B^{t-k} - T_s^{t-1}\right]. \quad (2)$$

Equation 2 estimates the slow-response sensor temperature measurement by adding to the last temperature a correction that depends on a lagged weighted mean of current and past baseline temperatures. There are two adjustable parameters – an amplitude factor '*C*' and a lag index '*K*'.

Figure 4 shows the error variance of the difference between the measurements of temperature by the slow-response sensor and calculations of the slow-response sensor-measured temperature for 21 March 2003 for choices of $C = 0.050$ and $C = 0.035$. The minimum variance for both curves occurs for lag $K = 2$. Figure 5 shows that the distribution of error variance for lag 2 is a minimum at $C = 0.035$.

Smoke temperature measurements for 12 February 2003 provided an independent dataset for testing Eqn 2. Figure 6 shows temperatures measured with the thermocouple (solid line) and the slow-response sensor (dashed line) for a hot smoke. The approximation to the slow-response temperature as calculated from Eqn 2 is given by the dotted line.

For the whole dataset, the variance between temperatures measured by the slow-response sensor and temperatures calculated by Eqn 2 was 0.019, giving a standard deviation of 0.13°C. The maximum point departure of temperature of

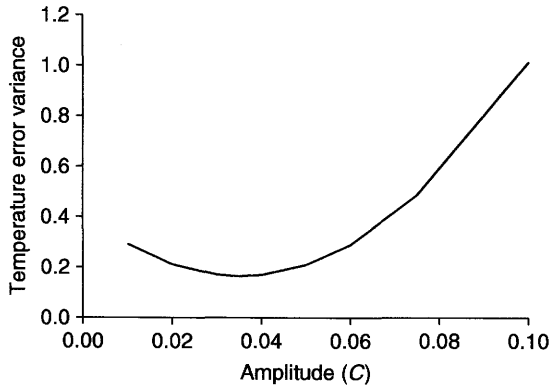

Fig. 5. The distribution of error variance as a function of amplitude (C) at lag 2.

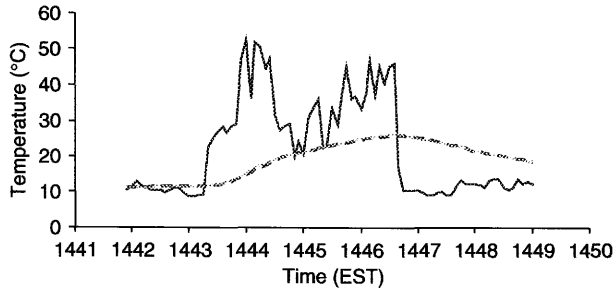

Fig. 6. Temperature (solid line – thermocouple; dashed line – slow-response; dotted line – calculated slow-response) for a smoke measured on 12 February 2003.

either sign was 0.54°C. Following the success with the independent 12 February dataset, Eqn 2 was used to reconstruct the slow-response temperatures for 18 March 2002.

The slow-response temperature and relative humidity were used to calculate the mixing ratio, a measure of the mass of water vapor present to the mass of dry air containing the vapor (Hess 1959). The mixing ratio does not suffer from the problems encountered with the Vaisala instrument described in Fig. 2. Graphs were created to display the fast-response temperature and the mixing ratio for each of the 27 smoldering smokes. The fast-response temperature showed when the instrument was inserted into the smoke and how hot the smoke was. The mixing ratio showed whether the smoke was drier or wetter than ambient air.

Results

Figure 7 shows fast-response temperature (T) and mixing ratio (MR) for three smokes on the Oconee National Forest on 6 March 2002. This was an unusually dry day with the ambient temperature around 20°C and ambient relative humidity of ~15%. During the sampling of smoke 1 (Fig. 7*a*), beginning at approximately 3 min after 1440 EST, the MR decreased slightly, suggesting that the smoke was slightly drier than the ambient air. Unless smoke is a moisture sink, smoke cannot be drier than ambient air. However, ambient MRs for the

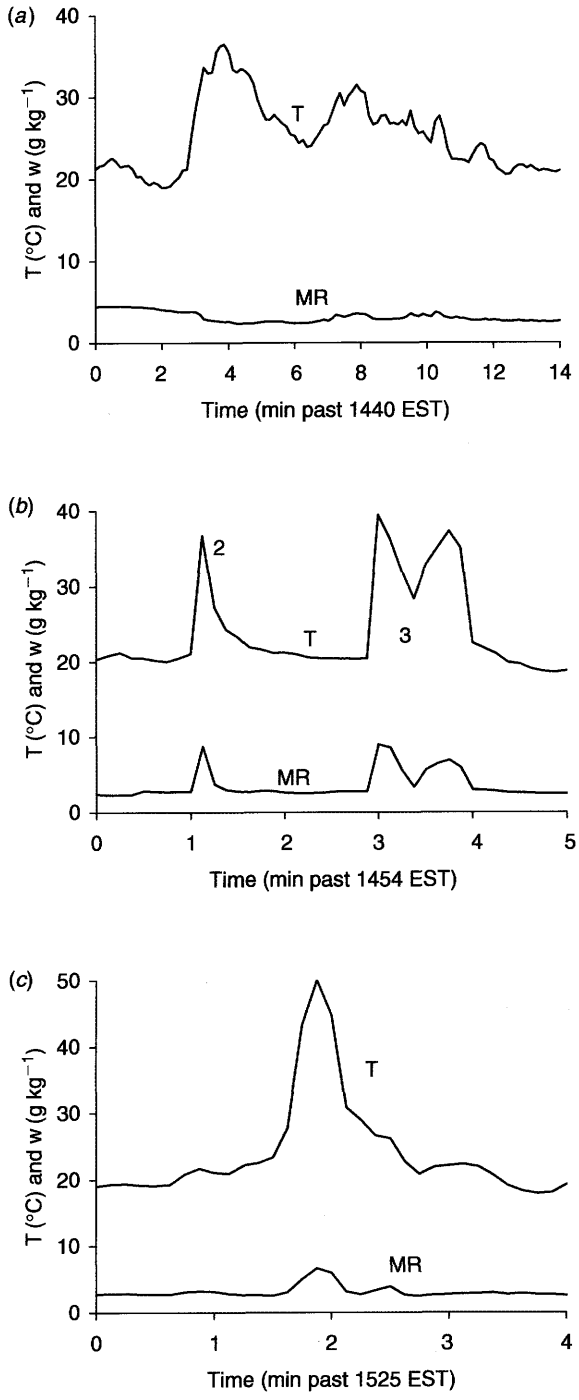

Fig. 7. Temperature via thermocouple (T) and mixing ratio (MR) for (*a*) smoke 1, (*b*) smokes 2 and 3, and (*c*) smoke 4 at the Oconee National Forest on 6 March 2002.

remainder of the sampling period were ~2.8 g kg^{-1}, meaning that the pre-smoke measurement ambient MR of 4.5 g kg^{-1} was anomalous.

Smokes 2 and 3 (Fig. 7*b*) produced moisture increases at each insertion of the instrument into the smoke, at approximately 1 and 3 min past 1454 EST. Mixing ratios jumped from

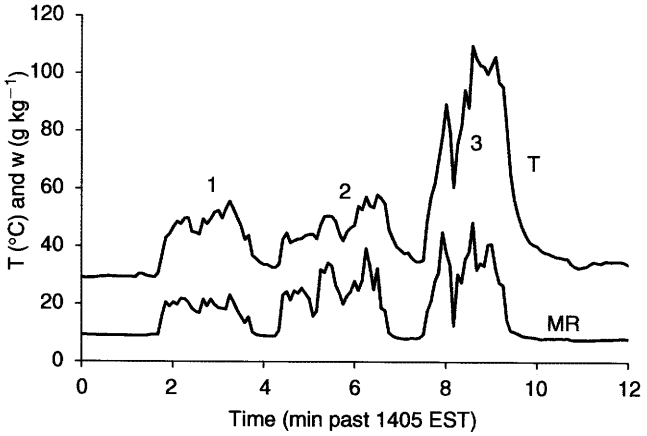

Fig. 8. Temperature via thermocouple (T) and mixing ratio (MR) for smokes 1–3 at the Hitchiti Experimental Forest on 18 March 2002.

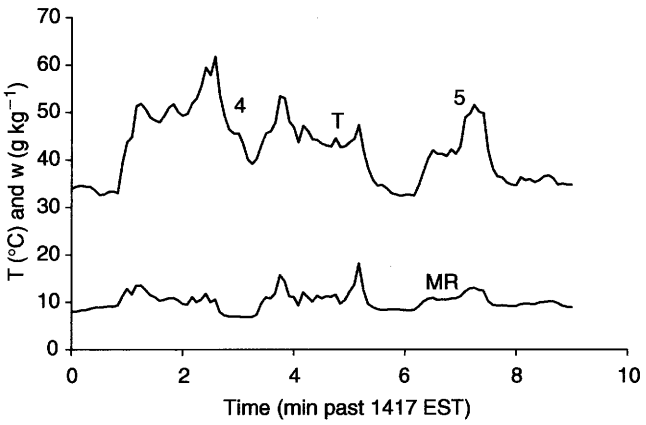

Fig. 9. Temperature via thermocouple (T) and mixing ratio (MR) for smokes 4–5 at the Hitchiti Experimental Forest on 18 March 2002.

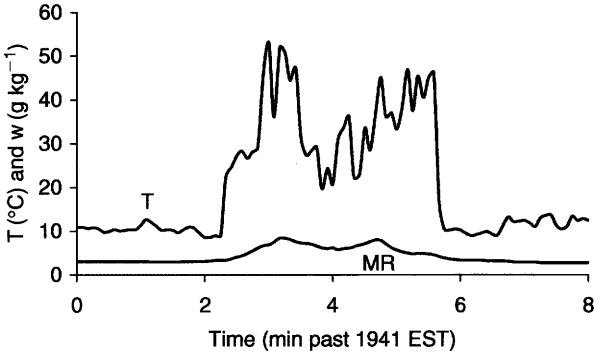

Fig. 10. Temperature via thermocouple (T) and mixing ratio (MR) for smoke 1 at the Francis Marion National Forest on 12 February 2003.

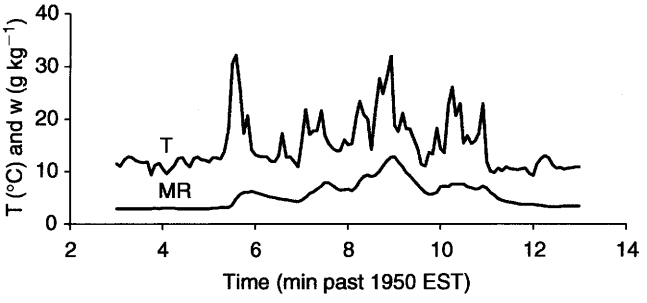

Fig. 11. Temperature via thermocouple (T) and mixing ratio (MR) for smoke 2 at the Francis Marion National Forest on 12 February 2003.

ambient (2.8 g kg^{-1}) to 8.8 g kg^{-1} and 8.6 g kg^{-1}, respectively. A small peak in MR (6.6 g kg^{-1}) was observed for smoke 4 (Fig. 7*c*).

The most extensive dataset on the temperature and moisture of smoldering smokes was collected at the Hitchiti Experimental Forest in central Georgia on 18 March 2002. Twenty-one smokes were sampled over a period of 90 min following a small experimental burn on a 0.64 ha plot. The ambient temperature was 31°C at the start of the experiment and 28°C by the end. The ambient relative humidity measured before entering the plot was 35%, and was 36% after exiting the plot. Most of the smokes were from logs. Other smokes were from light woody debris and stumps.

Figure 8 shows T and MR for the first three smokes on the Hitchiti Experimental Forest. Smoke 3 was the hottest measured for all smokes with a temperature of 109.8°C. Smoke 3 also had the highest moisture content with an MR of 48.4 g kg^{-1}. All three smokes could be considered 'moist' when compared with the ambient MR. MR jumped from the ambient MR (9.65 g kg^{-1}) to 21.8 g kg^{-1} for smoke 1, 34.3 g kg^{-1} for smoke 2, and 48.4 g kg^{-1} for smoke 3. These moist smokes should be compared with smokes 4–5 (Fig. 9), which represent the dry extreme for 18 March 2002. These smokes carried some additional moisture (18.2 g kg^{-1} and 13.0 g kg^{-1} respectively) but most MRs for smokes 4–5 were in the range 10–12 g kg^{-1}.

The 2002 data were collected during the afternoon on the Piedmont, a hilly, well-drained area in central Georgia. Smoke data on 12 February 2003 were collected at night in the Francis Marion National Forest on the flat Coastal Plain near Charleston, South Carolina. Both smokes originated in stumps. Figure 10 shows T and MR for smoke 1. Although the smoke was wetter than the ambient air (smoke MR was 8.4 g kg^{-1} *v.* 3.1 g kg^{-1} ambient MR), the event was relatively dry when compared with the measurements taken on 18 March 2002. Smoke 2 (Fig. 11) produced a maximum MR of 12.8 g kg^{-1} – four times larger than the ambient mixing ratio.

Table 1 summarizes 63 measurements taken within the 27 smokes. Moisture excess (g kg^{-1}) is the calculated addition of moisture beyond that of the ambient air. Moisture excesses range from nearly nothing to almost 39 g kg^{-1}. Figure 12 summarizes moisture excess by 5 g kg^{-1} categories. Forty-one percent of the moisture excesses exceed 10 g kg^{-1}. Once the MRs for the smokes had been calculated, a better estimate of the smoke relative humidity could be calculated

Table 1. Summary of temperature (T), mixing ratio (MR), and smoke relative humidity (RH) for 63 measurements of the 27 smokes

Date (yymmdd)	Time (EST)	Smoke no.	Ambient T (°C)	Smoke T (°C)	Ambient MR ($g\,kg^{-1}$)	Smoke MR ($g\,kg^{-1}$)	Moisture excess	Smoke RH (%)
020306	1444	1	20.3	37.0	2.42	2.42	0.00	6
	1455	2	20.3	36.7	2.42	8.78	6.36	23
	1457	3	20.3	39.5	2.42	9.00	6.58	21
	1457	3	20.3	37.3	2.42	6.93	4.51	18
	1458	3	20.3	32.0	2.42	5.53	3.11	19
	1527	4	19.9	50.1	2.66	6.65	3.99	9
020318	1407	1	31.1	46.7	9.66	20.60	10.94	32
	1407	1	31.1	49.8	9.66	20.48	10.82	27
	1408	1	31.1	49.6	9.66	21.66	12.00	29
	1408	1	31.1	55.7	9.66	23.17	13.51	23
	1409	2	31.1	42.1	9.66	24.70	15.04	49
	1410	2	31.1	50.6	9.66	34.32	24.66	44
	1410	2	31.1	45.2	9.66	22.80	13.14	39
	1411	2	31.1	57.4	9.66	39.40	29.74	37
	1411	2	31.1	54.3	9.66	33.51	23.85	36
	1413	3	31.1	78.6	9.66	45.09	35.43	16
	1413	3	31.1	89.5	9.66	38.30	28.64	9
	1413	3	31.1	81.9	9.66	27.70	17.54	9
	1414	3	31.1	94.4	9.66	35.70	26.04	7
	1414	3	31.1	109.8	9.66	48.40	38.74	6
	1414	3	31.1	99.9	9.66	40.81	30.75	7
	1419	4	31.1	51.3	9.66	13.50	3.84	17
	1420	4	31.1	51.7	9.66	10.90	1.24	13
	1421	4	31.1	51.8	9.66	13.56	3.90	16
	1422	4	31.1	53.4	9.66	15.75	6.09	18
	1424	5	31.1	47.3	9.66	18.60	8.94	28
	1424	5	31.1	51.5	9.66	13.30	3.64	16
	1427	6	31.1	43.4	9.66	13.01	3.35	24
	1427	6	31.1	49.8	9.66	15.29	5.63	21
	1428	6	31.1	49.4	9.66	14.68	5.02	20
	1429	7	31.1	65.5	9.66	21.24	11.58	14
	1429	7	31.1	51.0	9.66	15.80	6.14	20
	1430	7	31.1	49.5	9.66	11.02	1.36	15
	1433	8	31.4	40.0	8.02	20.75	12.73	46
	1434	8	31.4	40.8	8.02	27.70	19.68	59
	1436	9	31.4	51.5	8.02	18.25	10.23	23
	1437	9	31.4	50.0	8.02	15.46	7.44	21
	1443	10	31.4	56.8	8.02	26.63	18.61	25
	1443	10	31.4	57.0	8.02	25.18	17.16	24
	1445	11	31.4	56.1	8.02	23.98	15.96	24
	1445	11	31.4	55.0	8.02	31.42	23.40	33
	1512	12	31.4	40.7	8.02	11.73	3.71	25
	1512	12	31.4	42.3	8.02	12.16	4.14	24
	1513	13	31.4	44.1	8.02	18.09	10.07	32
	1514	13	31.4	42.8	8.02	15.35	7.33	29
	1514	13	31.4	40.4	8.02	17.05	9.03	37
	1515	13	31.4	41.3	8.02	13.94	5.92	29
	1516	14	28.3	44.0	8.56	16.39	7.83	30
	1519	15	28.3	51.7	8.56	15.51	6.95	19
	1521	16	28.3	60.7	8.56	13.34	4.78	11
	1524	17	28.3	54.0	8.56	13.89	5.33	15
	1527	19	28.3	70.0	8.56	17.02	8.46	9
	1527	19	28.3	79.9	8.56	20.13	11.57	7
	1529	20	28.3	67.5	8.56	17.60	9.04	10
	1532	21	28.3	44.5	8.56	22.62	14.06	40
	1533	21	28.3	42.1	8.56	18.67	10.11	37
030212	1943	1	10.4	50.8	3.10	8.40	5.30	11
	1944	1	10.4	45.1	3.10	7.90	4.80	13
	1945	1	10.4	40.5	3.10	4.90	1.80	11
	1956	2	10.4	21.0	2.90	7.20	4.30	47
	1957	2	10.4	24.8	2.90	11.00	8.10	58
	1959	2	10.4	32.0	2.90	12.80	9.90	44
	2001	2	10.4	26.1	2.90	7.60	4.70	37

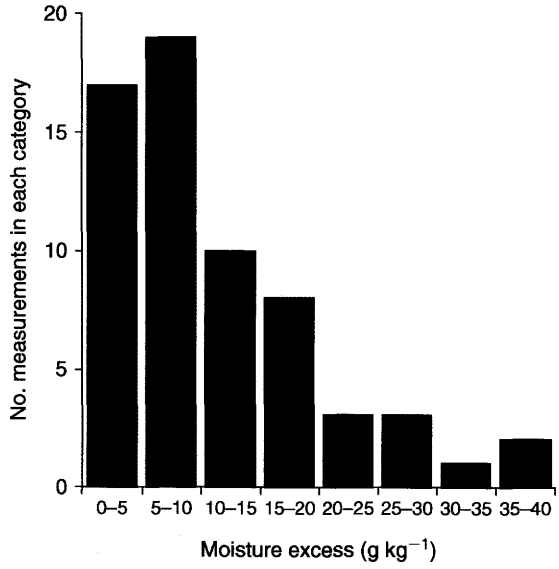

Fig. 12. Smoke moisture excess by 5 g kg^{-1} categories.

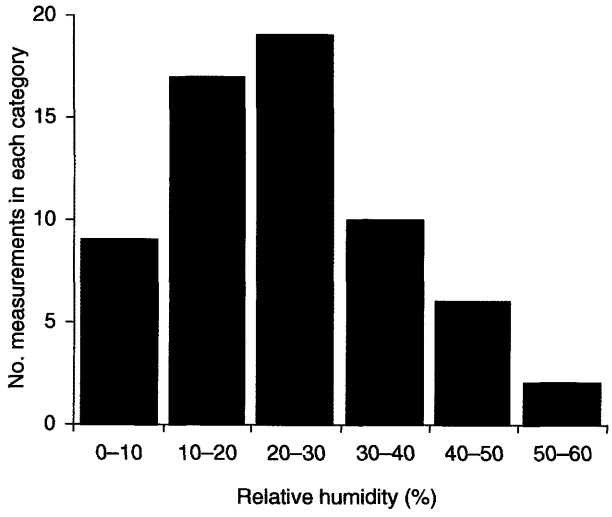

Fig. 13. Smoke relative humidity by 10% categories.

from temperatures measured by the fast-response thermocouple. Smoke relative humidity is given in the last column of Table 1. This ranges from very dry (6%) to moderately moist (59%). Figure 13 summarizes smoke relativity humidity by 10% categories. Here 59% of the smoke measurements fall into the relatively dry 10–30% categories.

The results presented in Table 1 are valid to the extent that the Vaisala HMP45AC temperature–humidity probe was in calibration and was capable of measuring high relative humidities at high temperatures typical of those found in the smokes observed during the present study. To test whether the large moisture excesses were real and not an artifact of the instrument, 17 smoke measurements at the high end of the temperature scale were submitted for calibration (Vaisala 2006). The calibration is summarized in Table 2.

Table 2. Calibration of the Vaisala HMP45AC temperature and relative humidity (RH) instrument used for the present study against a reference standard for 17 data points from the smoke moisture study

Point	Calibration		HMP45AC	
	Temperature (°C)	RH (%)	Temperature (°C)	RH (%)
1	43.9	51	43.6	48
2	44.7	54	44.4	52
3	45.6	75	45.3	73
4	46.8	60	46.5	58
5	48.0	49	47.7	47
6	48.8	17	48.5	15
7	49.8	41	49.5	38
8	50.6	36	50.3	33
9	51.8	43	51.4	41
10	53.1	44	52.8	41
11	54.6	51	54.3	49
12	56.2	31	55.9	28
13	57.9	31	57.5	28
14	59.5	28	59.1	25
15	61.0	32	60.7	29
16	62.4	30	62.0	27
17	63.8	22	63.4	20

The test chamber, a Thunder 2500 Two-Pressure Generator (Thunder Scientific, Albuquerque, NM, USA), was set to match within tolerance the 17 submitted temperature–relative humidity pairs. Then the readings of the HMP45AC were taken and compared with the reference measurements. The results showed that the temperature–relative humidity probe used for the present study was reading slightly cool (average error = −0.34°C) and slightly dry (average error = −2.67% relative humidity). All temperature and relative humidity errors were within tolerance.

Discussion

The measurements of moisture contained in 27 smokes in post-prescribed burn smoldering fuels reveal a wide range of moisture excesses. Adjacent smokes can be moist or dry. Factors such as the age, porosity, site (slope, surrounding material, ground exposure), length of time since the last rain, and where on the fuels the combustion is taking place determine the moisture content of the smoke. The largest moisture excess occurred with hottest smoke (smoke 3 on 18 March 2002). However, this was also the driest smoke (relative humidity = 6%).

Where does smoke moisture come from? The total moisture budget, MR_T, which was measured in the present study, is the sum of moisture contributed from the following sources:

$$MR_T = MR_a + MR_c + MR_f + MR_s + MR_L. \quad (3)$$

The first term, MR_a, is the moisture contained in ambient air. Unless smoke is a moisture sink, the total smoke moisture should never be less than that of the ambient air. During daytime when moisture within a well-mixed atmosphere is

spatially evenly distributed, MR_a can be calculated from temperature and relative humidity observed at nearby weather stations. However, at night under entrapment conditions, drainage flows may carry smoke into moist stream basins where standing water may be present to increase airmass moisture. Thus MR_a can be locally larger at night than that calculated from nearby weather stations. The second term, MR_c, represents moisture released as a product of the chemistry of combustion. The third term, MR_f, represents moisture evaporated from heated fuels that may or may not combust. Fuel type, fuel moisture, and fuel mass vary from smoke to smoke and thus contribute to the spatial variability of moisture observed in the smokes of the present study. The fourth term, MR_s, represents moisture evaporated from heated soils. Factors such as timing of the last rain and soil type – how much water is held near the surface – contribute to MR_s. Furthermore, Phillips and Marion (2004) showed that the composition of forest soils can vary over small spatial distances. MR_s may be a contributor to the spatial variability of moisture observed in the smokes of the current study.

The last term, MR_L, represents moisture added through atmospheric loading of moisture from smokes located upwind. Under conditions of entrapment that form at night under clear skies and light winds, moisture released from many smoldering smokes will be held near the ground. This moisture is available to be drawn into smokes located farther downwind. When large tracts of land are burned, MR_L may become large by the time air exits from the downwind boundary of the burned area. As regards the present study, all smokes on 18 March 2002 and 12 February 2003 were measured on small plots (0.64 and 1.0 ha, respectively). Inspection of the data revealed no evidence for atmospheric loading beyond the background noise in the data. The smokes measured on 6 March 2002 were located on a 417 acre (167 ha) tract. This burn was conducted during the afternoon under well-ventilated atmospheric conditions. Thus it is concluded that atmospheric loading was not a factor in any of the moisture excesses calculated for the present study.

Potter (2005) argued that water released during combustion (including fuel moisture) may produce moisture excesses in the range of 1–3 g kg^{-1}. Smaller water production should result from less complete smoldering combustion. However, the MR is the ratio of the mass of water released to the mass of dry air containing the water. The flaming stage develops strong convective currents that circulate large masses of air through the combustion area. Thus, for example, flaming combustion might release 6 g of water over a specified time during which 2 kg of air are circulated through the fire, yielding an MR of 3 g kg^{-1}. The cooler, oxygen-starved smoldering stage cannot develop strong convective currents at the ground. Thus, for example, smoldering combustion might release only 3 g of water over the same specified time but only 100 g of air might be circulated through the smoldering area yielding an MR of 30 g kg^{-1} – 10 times larger than that for flaming combustion. Therefore smoke moisture excesses calculated from smoldering fuels may be much larger than those suggested by Potter for flaming fuels.

Although moisture excesses released by smoldering smokes can be large, the net change of moisture within the mass of air departing from a burn site is unknown, although the impact will be to increase the moisture content of the air. Consider residual smoke coming from a rectangular-shaped tract of land with dimensions given by x and y, and the wind blowing in the x-direction. The MR flux (F_S) for all smokes in the tract is given by

$$F_S = MR_T \pi r^2 w \rho_s A, \tag{4}$$

where MR_T is the measured total smoke MR, r is the radius of the smoke, w is the smoke injection velocity, ρ_s is the number of smokes per unit area, and A is the area of the block burned. The MR flux (F_A) for ambient air in the absence of residual smoke is

$$F_A = MR_A yzu, \tag{5}$$

where MR_A is the measured MR for ambient air, z is the depth of the mixing layer above the tract, and u is the wind blowing along the x-direction of the tract. On departure from the burn area, the final MR flux (F_F) is therefore

$$F_F = MR_F yzu = MR_A(yzu - \pi r^2 w \rho_s A) + MR_T \pi r^2 w \rho_s A. \tag{6}$$

Here the total volume flux for the smokes is subtracted from the volume flux for ambient air because no new air enters the system. The smokes draw from existing ambient air. The final smoke MR is:

$$MR_F = MR_A + \frac{\pi r^2 w \rho_s x}{zu} MR_E, \tag{7}$$

where MR_E is the average of the moisture excesses ($MR_T - MR_A$) shown in the next to last column of Table 1.

Equation 7 estimates the contribution of smoke moisture to the ambient air departing the burn site. That contribution is large if the number and size of the smokes are large, the tract burned is large, the depth of the mixing layer is small, and the winds blowing across the burned tract are light. The latter two conditions are most likely to occur at night. For the 'typical' smoke, let $r = 30$ cm, $w = 1.0$ m s^{-1}, $\rho_s = 0.01$ m^{-2} (one smoke per 100 m^2). This combination yields a coverage of smoldering smokes equal to 0.28% of the tract burned. Let daytime wind and mixing heights be represented by $u = 5.0$ m s^{-1} and $z = 1000$ m, and nighttime conditions by $u = 1.0$ m s^{-1} and $z = 10$ m. For convenience, let the tracts burned be square in shape. Table 3 shows calculated moisture increases for ambient air departing the burn sites. Average smoke moisture excesses for each burn were calculated from the moisture excesses given in Table 1. All of the daytime moisture increases are tiny fractions of ambient

Table 3. Calculated moisture increases ($g\,kg^{-1}$) for daytime and nighttime weather conditions based on Eqn 7

Date	Block size (ha)	Average smoke moisture excess ($g\,kg^{-1}$)	Daytime ($g\,kg^{-1}$)	Nighttime ($g\,kg^{-1}$)	Additional ($g\,kg^{-1}$)
6 Mar 2002	167	4.9	3.5×10^{-3}	1.77	0.50
18 Mar 2002	0.64	12.7	5.7×10^{-4}	0.28	1.30
12 Feb 2003	1.0	4.0	2.2×10^{-4}	0.11	2.10
12 Feb 2003	1.0	7.6	4.3×10^{-4}	0.21	2.10

MR and thus would have negligible impact toward increasing the likelihood of fog.

However, at night, the relative humidity increases as the temperature falls. Thus if fog is going to present, it should be found at the lowest temperature, usually just before sunrise. For the three burn days, the temperatures and relative humidities at 0700 EST the morning following the burns were, respectively, 1°C and 87%, 16°C and 88%, and 2°C and 51%. The additional moistures needed to increase the relative humidities to 100% are shown in the last column of Table 3. Thus, for 6 March 2002, the additional moisture to bring the ambient air to saturation is only $0.5\,g\,kg^{-1}$. Yet Table 3 also shows that the additional moisture supplied by smoldering smokes to the ambient air leaving the burn site was $1.77\,g\,kg^{-1}$ – far more moisture than needed to bring the ambient air to saturation – assuming smoldering is represented by the conditions specified for Eqn 7. For the remaining events, the addition of moisture by smoldering smokes would not have been sufficient to saturate the ambient air.

The estimates from Eqn 7 show that the impacts of moisture from smoldering smokes on ambient conditions are not insignificant. The additional moisture is available to increase the density of existing fog or to trigger fog in areas where fog might otherwise not have occurred.

The prevailing hypothesis for the formation of smoke and fog from entrapped woodland smoke argues for increased fog density as a consequence of competition for the available water between an enormous number of condensation nuclei released in smoke. The outcome is a large number of small diameter fog droplets. These are more effective scatters of light than are a smaller number of large diameter fog droplets. To the prevailing hypothesis must be added the cumulative moisture released over a landscape to the atmosphere through smoldering combustion, moisture that is available to trigger fog and to further increase the number of fog droplets.

Acknowledgements

Mr Ken Forbus and Mr Tim Giddens of the USDA Forest Service, Forestry Science Research Laboratory, Athens, GA, USA, are acknowledged for their contributions to equipment management and field measurements. The project was conducted as part of the Southern Regional Models for Predicting Smoke Movement Project (01.SRS.A.5) funded by the USDA Forest Service National Fire Plan.

References

Achtemeier GL (2005) Planned burn – Piedmont. A local operational numerical meteorological model for tracking smoke on the ground at night: model development and sensitivity tests. *International Journal of Wildland Fire* **14**, 85–98. doi:10.1071/WF04041

Achtemeier GL, Glitzenstein J, Naeher L (2006) Measurements of smoke from chipped and unchipped plots. *Southern Journal of Applied Forestry*, in press.

Hess SL (1959) 'Introduction to theoretical meteorology.' (Holt and Company: New York)

Kokkola H, Romakkaniemi S, Laaksonen A (2003) On the formation of radiation fogs under heavily polluted conditions. *Atmospheric Chemistry and Physics* **3**, 581–589.

Lavdas LG (1996) Improving control of smoke from prescribed fire using Low Visibility Occurrence Risk Index. *Southern Journal of Applied Forestry* **20**, 10–14.

Lavdas LG, Achtemeier GL (1995) A fog and smoke risk index for estimating roadway visibility hazard. *National Weather Digest* **20**, 26–33.

Mobley HE (1989) Summary of smoke-related accidents in the South from prescribed fire (1979–1988). Technical Release 90-R-11. (American Pulpwood Association)

Phillips JD, Marion DA (2004) Pedological memory in forest soil development. *Forest Ecology and Management* **188**, 363–380. doi:10.1016/J.FORECO.2003.08.007

Potter B (2005) The role of released moisture in the atmospheric dynamics associated with wildland fires. *International Journal of Wildland Fire* **14**, 77–84. doi:10.1071/WF04045

Vaisala (2006) Certificate of calibration. Report 072006-W2340091-RH. (Vaisala: Boston)

Wade DD, Brock BL, Brose PH, Grace JB, Hoch GA, Patterson WA (2000) Fire in eastern ecosystems. In 'Wildland fire in ecosystems: effects of fire on flora'. (Eds JK Brown, JK Smith) pp. 53–96. USDA Forest Service, Rocky Mountain Research Station General Technical Report RMRS-42. (Ogden, UT)

Ward DE, Hardy C (1991) Smoke emissions from wildland fires. *Environment International* **17**, 117–134. doi:10.1016/0160-4120(91)90095-8